Biosynthesis and characterization of Cu/ZnO nanocomposite using *lantana aculeate* leaf extract: Evaluation of antioxidant, antibacterial and cytotoxic activity

P. Baby Shakila, S. Narendhran*, NT. Arishiya and D. Naveen Kumar

Department of Biotechnology, Sri Krishna Arts and Science College, Kuniamuthur, Coimbatore – 641 008

*Corresponding mail ID: narendhrans@skasc.ac.in

Abstract

In the current study, cytotoxic activity of copper-doped zinc oxide (Cu/ZnO) nanocomposite synthesized using *Lantana aculeate* was carried out. The phyto-mediated synthesized nanoparticle was subjected to various characterization analysis such as UV-Visible spectrophotometer, Fourier Transfer Infrared Spectroscopy (FTIR), Energy diffraction X-ray (EDX), X-Ray Diffraction (XRD), Particles size analysis and Scanning Electron Microscope. It was found that the characterized nanocomposite were spherical in shape without any aggregation. The result of MTT assay, confirmed the cytotoxic activity of Cu/ZnO nanocomposite against the SiHa cervical cancer cell line. The results of this current study directs that green synthesis of the Cu/ZnO nanocomposite using plant extract of *Lantana aculeate* have an ability to treat quite a lot of diseases, however, it enforces clinical studies to determine their prospective as anti-cancer agents.

Keywords: Copper, Cytotoxic activity, *Lantana aculeate,* Zinc oxide

Introduction:

Nanocomposite has now been an emerging field that gains huge attention all over the world in the field of science and technology (Hasan, 2015). These exclusive properties of nanocomposite has directed them in the path of providing its application in various aspects (Assessment R Nanoparticles in the Environment, 2007).The manufacturing of nanocomposite at the level of nanometer scale has now became an incipient interdisciplinary field. The fundamental properties of composite such as optical, electrical and mechanical can be expressed based on their structural order, size and composition (Caruso, 2001). In order to enhance the properties, method of synthesis have been developed and improved (Cho *et al.,* 2013). The synthesis of nanoparticles using chemical method shows adverse effects due to the presence of

some toxic elements. The alternative and eco- friendly method of synthesis by using microorganisms (Klaus *et al.,* 1999; Konishi *et al.,* 2007) and plant extracts (Shankar *et al.,* 2004; Ahmad *et al.,* 2011). This biological method can either be an intracellular or extracellular synthesis of nanocomposite; it helps to overcome the toxic effects caused by chemical and physical methods. (Vigneshwaran *et al.,* 2007; Hulakoti *et al.,* 2014).

Copper is a soft, malleable, non- toxic, inorganic and ductile metal. They have a very high electrical and thermal conductivity. It plays a substantial role in modern electronic circuits due to its low cost (Schapter *et al.,* 2004) and also significant role in sensor application. Due to its tremendous electrical conductivity, excellent compatibility and its catalytic behaviour, they have attracted the attention of scientists to use this nanoparticle in future nano-devices (Pergolese *et al.,* 2006). Copper nanoparticle synthesized using plant extract was found to be the most prominent method. (Bhattacharya *et al.,* 2006).

Zinc oxide has a much more attraction due to their potential application in various fields of science and technology (Klingshirn *et al.,* 2010). Zinc oxide at a level of nanoscale has wide range of application in food industry as a food preservative and found to show antimicrobial activity. Zinc oxide is now listed as a non- toxic material and can also be used in various food packing factories. It is recognized as a safe material by food and drug administration (FDA, 2011). In-order to improve the property of polymeric material, zinc oxide nanoparticles can be incorporated to deliver antimicrobial activity. The structure of the synthesized zinc oxide nanoparticles can be doping with some transition metals like cobalt, nickel, copper, manganese and iron. Among all these metals, copper has found to be significant with higher electrical conductivity and recorded as an important transition metal in doping (Allabergenov *et al.,* 2013; Dominic *et al.,* 2013).

ZnO and CuO nanoparticles show relatively high biocompatibility. Their bulkier form is generally recognized as safe (GRAS) by the FDA. Zinc is an important co-factor in various cellular mechanisms and plays an important role in maintaining cellular homeostasis; hence ZnO shows biocompatibility. The administered ZnO can be easily biodegraded or can take part in the active nutritional cycle of the body (Choudhury and Panda, 2004.). While extracellular ZnO shows biocompatibility,

elevated levels of administered intracellular ZnO show enhanced cytotoxicity through zinc-mediated protein activity disequilibrium and oxidative stress (Kahru and Dubourguier, 2010). CuO nanoparticles have the unique ability to induce oxidative stress in cancer cells, which has been found to be one of the mechanisms of cytotoxicity of CuO nanoparticles towards cancer cells. This property is due to the semiconductor nature of CuO. It induces ROS generation, leading to oxidative stress and eventually cell death when the anti-oxidative capacity of the cell is exceeded.

The basic mechanism behind the cytotoxicity of nanoparticles is the intracellular release of dissolved ions, followed by ROS induction. This event causes NPs mediated protein activity disequilibrium and oxidative stress, eventually killing the cell. Soluble extracellular zinc and copper shows very little cytotoxicity. Recent research shows that extracellular soluble zinc, when exposed to cell culture and media, forms poorly soluble amorphous zinc-carbonate phosphate precipitates (phosphate from media). This precipitate is supposed to protect the cell from the cytotoxicity of zinc (Kasemets *et al*., 2009). On the other hand, with the release of soluble copper ions inside the cell, a cascade of pathways interrelated to each other takes place, which is responsible for the cytotoxic response of the CuO nanoparticles.

Many in vitro studies have proved that NPs show selective cytotoxicity towards cancer cells. Hanley suggested that they show 28-35 times selective toxicity towards cancer cells compared with that of normal cells. This selective cytotoxicity in cancer cells in in-vitro condition can also be further exploited in the in vivo condition by selectively targeting nanoparticles towards cancer cells. NPs selectively kill cancer cells by inferring selective localization and selective cytotoxicity towards them. Previously, *L. aculeata* has been extensively investigated for the phytochemical screening. Several triterpenoids, napthaquinones, flavonoids, phenol compounds, alkaloids and glycosides were isolated from this plant (Ghisalberti, 2000). There has been an increasing incidence for biological synthesis of metal oxide nanocomposite.

In the present study, Cu doped ZnO nanocomposite were synthesized using aqueous extract of *Lantana aculeata* Linn leaves with a simple precipitation method for biological activity (Fig 1). The prepared samples were characterized by UV- Vis spectroscopy, Fourier transform infrared spectroscopy (FTIR), X-ray diffraction (XRD), Face emission scanning electron microscopy (FESEM), the purity of the

sample was tested by energy dispersive spectroscopy (EDS). To determine antioxidant activity of Cu/ZnO nanocomposite by DPPH method and antibacterial activity against *Ecoli* (MTCC: 912), *Bacillus subtilis* (MTCC: 121) and *Streptococcus pyrogenes* (MTCC: 1925) performed using well diffusion method.

MATERIALS AND METHODS

Materials

Fresh, healthy and young *L. aculeate* leaves were collected from Vadavalli region (11.0100° N, 76.9000° E), Coimbatore, Tamil Nadu, India. The sample was authenticated by Botanical Survey of India, Coimbatore (BSI/SRC/5/23/2014-15/Tech/1418). SiHa cell lines were purchased from NCCS Pune. All chemicals were purchased from Sigma-Aldrich chemicals, India.

Preparation of plant sample and synthesis of ZnO nanoparticles

Powdered *L*. *Aculeate* (5 g) was boiled in 100ml of distilled water for 15min and then filtered with Whatmann filter paper. The extract was then filtered using Whatmann No.1 filter paper. 0.1 M Zinc nitrate was prepared with 90 ml of de-ionized water. After complete dissolution of zinc nitrate, the flask containing the solution was heated on a water bath at 80°C for 5–10 min. Then, the zinc nitrate solution was mixed in 10 ml of plant extract under constant stirring. This mixture of the solution was kept at 100 ˚C for 5h, under vigorous stirring. This precipitate was discarded through centrifugation (7000 rpm for 15 min). Finally, a brown color change to the solid pale yellow color precipitate was derived. The precipitate was purified through washing with de-ionized water followed by methanol and air dried. This product was annealed at 400 ˚C for 2 h. At the end, white color powder was obtained.

Synthesis of Cu/ZnO nanocomposite

0.1 mM copper sulphate was prepared with de-ionized water and the volume was made up to 250 ml. After complete dissolution of precursors, the flask containing the solution was heated on a water bath at 80°C for 5–10 min. Then, precursor's solution was mixed in plant extract and 0.5 g of zinc oxide nanoparticles under

constant stirring. This mixture of the solution was kept at 100 ˚C for 5h, under vigorous stirring. The precipitate was purified through washing with de-ionized water followed by methanol and air dried. This product was annealed at 400 ˚C for 2 h. At the end, black powder was obtained.

Characterization of nanocomposite

Optical properties of synthesized Cu/ZnO nanocomposite were confirmed by Ultra Violet–visible spectroscopy (UV vis) (UV-2450, Shimadzu) in 200–800 nm wave length range. Fourier transform infrared (FT-IR) spectrometer was used to analysis of functional groups in the synthesized Cu/ZnO nanocomposite. FT-IR spectra were recorded in the range 4000–400cm-1 (Perkin-Elmer 1725x), by KBr pellet method. Elemental analysis of Cu/ZnO by energy dispersive X-ray spectrometer (EDX) (RONTEC's EDX system, Model QuanTax 200, Germany). Particle sizes were analyzed using PSA (Horiba) at 90^{o}C respectively. 2D structure of the synthesized Cu/ZnO nanocomposite were carried out by X-ray diffractometer (Perkin-Elmer spectrum one instrument) Cu-Kα radiations (λ = 0.15406 nm) in 2θ range from 20° to 80°. 3D Structure of the synthesized Cu/ZnO nanocomposite was characterized by scanning electron microscope (SEM) (Model JSM 7610F, JOEL, USA).

Antioxidant and Antibacterial activity of Cu/ZnO nanocomposite

Antioxidant activity of Cu/ZnO nanocomposite by DPPH radical scavenging activity was analyzed according to method described by Narendhran et al. [21], in which DPPH (0.1mM) reagent taken as a control and ascorbic acid used as standard (lower the absorbance indicates higher the free radical scavenging activity). Then the absorbance of the reaction mixture read at 517 nm with a Shimadzu UV-2450 spectrophotometer. The antioxidant data were analyzed at the significant level $P \leq 0.05$ by t test to identify different between nanocomposite concentrations. Antibacterial activity of *L. aculeate* mediated Cu/ZnO nanoparticles were determined by well diffusion method. Bacterial culture swapped on nutrient agar plate and 5mm size of well punched on agar surface with help of sterile gel puncher. Various concentration of Cu/ZnO nanocomposite such as 25, 50, 75, 100 mg/L and tetracycline (positive control – 10 µg/ml) added in appropriate well. The plates were incubated at room temperature for 24 hours. The zone of inhibition were measured (millimeter in diameter) and mean ± standard deviation values are recorded. One

way analysis of variance (ANOVA) were also perform to test effect of Cu/ZnO nanocomposite dose on the test parameters. *P*-values of ≤ 0.05 were considered statistically significant.

Determination of *in vitro* anti-proliferative effect of *Lantana aculeate* mediated Cu/ZnO nanocomposite on cultured SiHa cell lines

SiHa cell lines were purchased from NCCS Pune were maintained in Dulbecco's modified eagles media (HIMEDIA) supplemented with 10% FBS (Invitrogen) and grown to confluency at 37°C in 5 % CO2 in a humidified atmosphere in a CO2 incubator (NBS, EPPENDORF, GERMANY). The cells were trypsinized (500µl of 0.025% Trypsin in PBS/ 0.5mM EDTA solution (Himedia)) for 2 minutes and passaged to T flasks in complete aseptic conditions. Extracts were added to grown cells at a final concentration of 6.25 µg/ml, 12.5 µg/ml, 25 µg/ml, 50 µg/ml and100 µg/ml from a stock of 1mg/ml and incubated for 24 hours.

The % difference in viability was determined by standard MTT assay after 24 hours of incubation. MTT is a colorimetric assay that measures the reduction of yellow 3-(4, 5dimethythiazol- 2-yl)-2, 5-diphenyl tetrazolium bromide (MTT) by mitochondrial succinate dehydrogenase. The MTT enters the cells and passes into the mitochondria where it is reduced to an insoluble, colored (dark purple) formazan product. The cells are then solubilized with an organic solvent Dimethyl sulfoxide (Himedia) and the released, solubilized formazan product was measured at 540nm. Since reduction of MTT can only occur in metabolically active cells, the level of activity is a measure of the viability of the cells. The cells was washed with 1x PBS and then added 30 µl of MTT solution to the culture (MTT -5mg/ml dissolved in PBS). It was then incubated at 37^{o}C for 3 hours. MTT was removed by washing with 1x PBS and 200µl of DMSO was added to the culture. Incubation was done at room temperature for 30 minutes until the cell was lysed and colour was obtained. The solution was transferred to centrifuge tubes and centrifuged at top speed for 2 minutes to precipitate cell debris. Optical density was read at 540 nm using DMSO as blank in a microplate reader (ELISASCAN, ERBA). The % viability was determined using following formula.

% viability = (OD of Test/ OD of Control) X 100

Results and Discussion

UV visible spectroscopy

The Cu/ZnO nanocomposite synthesised using simple precipitation method was characterised using UV-Vis absorption spectrum at 200 to 800nm. The absorption spectrum of the synthesized nanocomposite recorded the peak at 240 nm (Fig 2). Khan et al (2018) synthesized Cu/ZnO nanoparticles using simple precipitation method and observed wide range of optical density at 317nm. We concluded that band gap energy of biological synthesized nanoparticles are low when compared to chemical synthesis.

FTIR analysis

In order to determine the functional groups on *Lantana aculeata* Linn leaves extract and identify their role in the synthesis of Cu/ZnO nanocomposite by FTIR analysis. The peak in the region between 400 and 600 cm^{-1} is allotted to Cu-Zn [Tas et al., 2002]. In FTIR spectra of green synthesized Cu/ZnO nanocomposite are showed in the Fig 3. The spectrum showed band at 426 and 516 cm^{-1}corresponding to metal-oxide (M-O). The band in the region of 1516 cm^{-1} and 1741 cm^{-1} can be assigned to N-O asymmetric and C=O stretching vibration respectively. The distinguished peak was observed in the region 3421 cm^{-1}, attributed to OH stretching of water molecules in Cu/ZnO nanocomposite. Nitro and Ketone are the functional groups that is responsible for the synthesis of Cu/ZnO nanocomposite.

XRD analysis of synthesized nanoparticles

X ray diffraction study was carried out for the synthesized nanoparticle to confirm their phase. The Cu/ZnO nanocomposite are corresponding to the crystal plane of (100), (002), (101), (102), (110), (103), (200), (112), (201), (004) and (202) found to match with JCPDS-06-2151 (Fig 4). The standard diffraction peak reveal that crystal nature of nanocomposite is hexagonal wurtzite structure. Bhuyan et al 2015 [17] explained mechanical assisted thermal decomposition process for synthesis of Cu/ZnO nanocomposite using zinc acetate and copper acetate that cannot control the crystal structure of Cu doped with ZnO. Ahmad Khan et al. [2017] explained the crystal nature of Cu/ZnO NPs synthesized from leaf extract of *Abutilon indicum* and *Clerodendrum inerme* with grain size of 17 and 20 nm respectively.

Thutiyaporn *et al.,* 2018 synthesized Cu/ZnO nanocomposite by co-precipitation method using copper ion at various doping concentration which is annealed at 500ºC. The undoped nanoparticles showed hexagonal structure whereas, zinc oxide nanoparticles doped with different concentration of copper ion are found to correlate with the crystalline orientation planes. We revealed that the radii of copper ion is closed to that of the zinc ion so, the penetration of copper into the composite of zinc oxide is easy during the synthesis process. Instead of chemical synthesis, plant mediated nanocomposite can control the crystal structure.

EDX, FESEM and Particle analysis of the Cu/ZnO nanocomposite

To confirm the elemental composition of the synthesized Cu/ZnO nanocomposite by EDX analysis. The purity of nanoparticles is confirmed by the indication of strong signal from Cu, Zn and O. EDX analysis of Cu/ZnO nanocomposite is 26.24 % of copper, 56.46 % of zinc and 17.30 % of oxygen, which confirms the elemental composition of CuO nanoparticles (Fig 5). The SEM images of Cu/ZnO nanocomposite are shown in Fig 6. From the images it is evident that the morphology of nanocomposite was spherical shaped and well distributed without aggregation, which is very similar to earlier studies (Ahmad Khan *et al*., 2017). From the results of particle size analysis, the average size of the synthesized Cu/ZnO nanocomposite was found to be 37 ± 6 nm (Fig 7).

Antioxidant and Antibacterial activity of Cu/ZnO nanocomposite

In DPPH assay, the biological activity of synthesized nanocomposite is significantly higher in concentration when compared with ascorbic acid. The results are expressed in Mean and statistically significant by using t-test (P≤0.05) (Table 1). *L. aculeate* mediated Cu/ZnO nanocomposite shows an excellent antibacterial activity against bacterial pathogenic (Table 2). Highest zone of inhibition observed in Cu/ZnO nanocomposite against *Streptococcus pyrogenes* with diameter of 16.66 ± 0.66 mm at a concentration 100 mg/ml and lowest inhibition obtained in *E.coli* with zone diameter 13.66 ± 2.08 mm at same concentration (Fig 8). *L. aculeate* mediated Cu/ZnO nanocomposite showed effective antibacterial activity in *E.coli*. Hassan et al (2017) reported that excellent antimicrobial properties of Cu doped ZnO nanoparticles against *E.coli* due to free radical. Khan et al (2018) explained the

antibacterial activity of Cu doped ZnO NPs are effective when compared to un-doped ZnO nanoparticles against *Bacillus sp*.

Cytotoxic study of Cu/ZnO nanocomposite on SiHa cell line

The cytotoxicity of the Cu/ZnO nanocomposite was evaluated against SiHa cell lines at a various concentration (6.5–100 µg/ml). Table 3 shows the cytotoxic activity of Cu/ZnO nanocomposite. IC_{50} value was calculated for the cytotoxic effect of Cu/ZnO nanocomposite was found to be 37.47 µg/ml. Ru Yuan et al., 2016 concluded that Zn/CuO nanocomposite could inhibit cell proliferation, induced apoptosis and cell arrested at G2/M phase.

Conclusion

The biological method of nanocomposite synthesis using plant extract has promoted the development of an advanced nanomaterials. This green synthesis of nanoparticle are found to be an eco-friendly option to replace the physical and chemical method of synthesis. The simple biological method had been followed for the synthesis of the Cu/ZnO nanocomposite using the plant extract of *Lantana aculeate*. The nanocomposite synthesized were characterized were found to be spherical shape with 37 ± 6 nm size. L. aculeate mediated Cu/ZnO nanocomposite have excellent antioxidant and antibacterial activity against *S. pyrogenes.* The cytotoxic assay of *Lantana aculeate* mediated Cu/ZnO nanocomposite were assessed against SiHa cell line. The cytotoxic assay demonstrated that the Cu/ZnO nanocomposite showed the best result against SiHa cell line in an *in vitro* condition. The current study suggested that biological synthesized Cu/ZnO nanocomposite should be potentially used in cancer therapy.

Acknowledgment

The authors is grateful to Tamil Nadu State Council for Science and Technology (TNSCST), DOTE Campus, Chennai, India for sanctioning the financial assistant and management of Sri Krishna Arts and Science College, Coimbatore, India for providing necessary facilities to carry out this study.

REFERENCE:

1. Caruso, F. AdV. Mater. 2001, 13, 11.
2. Hasan S 2015 A Review on Nanoparticles : Their Synthesis and Types Biosynthesis : Mechanism 4 9–11.
3. Assessment R 2007 Nanoparticles in the Environment.
4. Machado S, Pacheco J G, Nouws H P A, Albergaria J T and Delerue-Matos C 2015 Characterization of green zero-valent iron nanoparticles produced with tree leaf extracts Sci. Total Environ. 533 76–81.
5. Cho E J, Holback H, Liu K C, Abouelmagd S A, Park J and Yeo Y 2013 Nanoparticle characterization : State of the art , challenges , and emerging technologies.
6. Klaus T., Joerger R., Olsson E. and Granqvist C.G., SilverBased Crystalline Nanoparticles, Microbially Fabricated, J. Proc. Natl. Acad. Sci. USA, 96, 13611-13614, (1999)
7. Konishi Y. and Uruga T., Bioreductive Deposition of Platinum Nanoparticles on the Bacterium Shewanella algae, J. Biotechnol., 128, 648-653, (2007).
8. Vigneshwaran N., Ashtaputre N.M., Varadarajan P.V, Nachane R.P., Paralikar K.M., Balasubramanya R.H., Materials Letters, 61(6), 1413-1418, (2007).
9. Shankar S.S., Ahmed A., Akkamwar B., Sastry M., Rai A., Singh A. Biological synthesis of triangular gold nanoprism, Nature, 3 482, (2004).
10. Ahmad N., Sharma S., Singh V.N.,. Shamsi S.F, Fatma A. and Mehta B.R., Biosynthesis of silver nanoparticles from Desmodium triflorum : a novel approach towards weed utilization, Biotechnol. Res. Int . 454090 (1-8), (2011).
11. Hulakoti N.I. and Taranath T.C., Biosynthesis of nanoparticles using microbes: A Review. Colloids surf Bio Interfaces, (121), 474-83, (2014).
12. Mann S., Biomineralization, Principles and Concepts in Bioinorganic Materials Chemistry, Oxford University Press, Oxford, UK, (2001).
13. Schapter, A.K., Hu, H., Grenier, A., Schneider, R., Philips, F., 2004. Appl. Phys. A Mater. Sci. Process. 78, 73–75.
14. Pergolese, B., Miranda Muniz, M., Bigotto, A., 2006. J. Phys. Chem. B 110, 9241–9247.
15. Bhattacharya, J., Choudhary, U., Biwach, O., Sen, P., Dasgupta, A., 2006. Nanomed. Nanotechnol. Biol. Med. 2, 191–199.

16. FDA (2011) Part 182—substances generally recognized as safe. Food and drug administration, Washington DC, USA. Available at: http://ecfr.gpoaccess.gov/cgi/t/text/text-idx? Accessed 28 March 2011.
17. Klingshirn C.F., Waag A., Hoffmann A., Geurts J.. Zinc oxide: from fundamental properties towards novel applications.Springer, Heidelberg (2010).
18. Dominic Bresser, Franziska Mueller, Martin Fiedler, Steffen Krueger, RichardKlo epsch, Dietmar Baither, Martin Winter, Elie Paillard, Stefano PasseriniTransition-metal doped zinc oxide nanoparticles as a new lithium-ion anode material Chem Mater, 25 (2013), p. 4977
19. Allabergenov B., Chung S.H., Jeong S.M., Kim S., Choi B. Enhanced blue photoluminescence realized by copper diffusion doping of ZnO thin films Opt Mater Exp, 3 (2013), p. 1733.
20. Gunalan Sangeetha , Sivaraj Rajeshwari , Rajendran Venckatesh ,2011. Green synthesis of zinc oxide nanoparticles by aloe barbadensis miller leaf extract: Structure and optical properties. Materials Research Bulletin 46 (2011) 2560–2566.
21. Paparazzo E (1992) Evidence of Si-OH species on the surface of aged silica. J Vac Sci Technol 10:2892–2896.
22. Ulrich A.B., Pour P.M., in Encyclopedia of Genetics, 2001.
23. Thutiyaporn Thiwawong , Korakot Onlaor , Natpasit Chaithanatkun, Benchapol Tunhoo, 2018. Preparation of Copper Doped Zinc Oxide Nanoparticles by Precipitation Process for Humidity Sensing Device.
24. Midander. K, Cronholm .P, Karlsson.H.L. “Surface characteristics, copper release, and toxicity of nano- and micrometer-sized copper and copper (ll) oxide particles: a cross-disciplinary study,” Small, vol. 5, no. 3, pp. 389–399, 2009.
25. Shuvasish Choudhury, Sanjib Kumar Panda, 2004. “Role of salicylic acid in regulating cadmium induced oxidative stress in *Oryza sativa* L. roots”, Bulg. J. Plant Physiol, 30(3-4), 95-110.
26. Anne Kahru, Henri-Charles Dubourguier, 2010. “From ecotoxicology to nanoecotoxicology”, Toxicology, 269, 105-119.
27. Kaja Kasemets, Angela Ivask, Henri-Charles Dubourguier, Anne Kahru, 2009. “Toxicity of nanoparticles of ZnO, CuO, TiO_2 to yeast *saccharomyces cerevisiae*”, Toxicology in vitro, 23, 116-1122.

28. Ghisalberti E.L, 2000. "*Lantana camara* L. (verbenaceae)", Fitoterapia, 71, 467-486.

29. Narendhran S, Manikandan M and Baby shakila P, 2019. "Antibacterial, antioxidant properties of *Solanum trilobatum* and sodium hydroxide mediated magnesium oxide nanoparticles: a green chemistry approach", Bull. Mater. Sci, 42:133.

30. Shakeel Ahmad Khan, Farah Noreen, Saida Kanwal, Ahsan Iqbal, Ghulam Hussain. "Green synthesis of ZnO and Cu-doped ZnO nanoparticles from leaf extracts of *Abutilon indicum, Cleodendrum infortunatum, Cleodendrum inerme* and investigation of their biological and photocatalytic activities", Materials science and engineering C (2017).

31. Iman A. Hassan, Sanjayan Sathasivam, Sean P. Nair and Claire J. Carmalt, 2017. "Antimicrobial properties of copper-doped ZnO coatings under darkness and white light illumination", ACS Omega, 2, 4556-4562.

32. Khan S. A, Noreen F, Kanwal S, Hussain G, 2017. "Comparative synthesis, characterization of Cu-doped ZnO mamoparticles and their antioxidant, antibacterial, antifungal and photocatalytic dye degradation activities", Digest journal of nanomaterials and biostructures, Vol. 12, No.3, p. 877-889.

33. Ru Yuan, Huanli Xu, Xiaohui Liu, Ye Tian, Cong Li, Xiaoliang Chen, Shuonan Su, Ilana perelshtein, Aharon Gedanken, Xiukun Lin, 2016. "Zinc-doped copper oxide nanocomposites inhibit the growth of human cancer cells through reactive oxygen species-mediated NF-$_k$B activation", ACS Applied Materials & Interfaces.

Figures and Tables

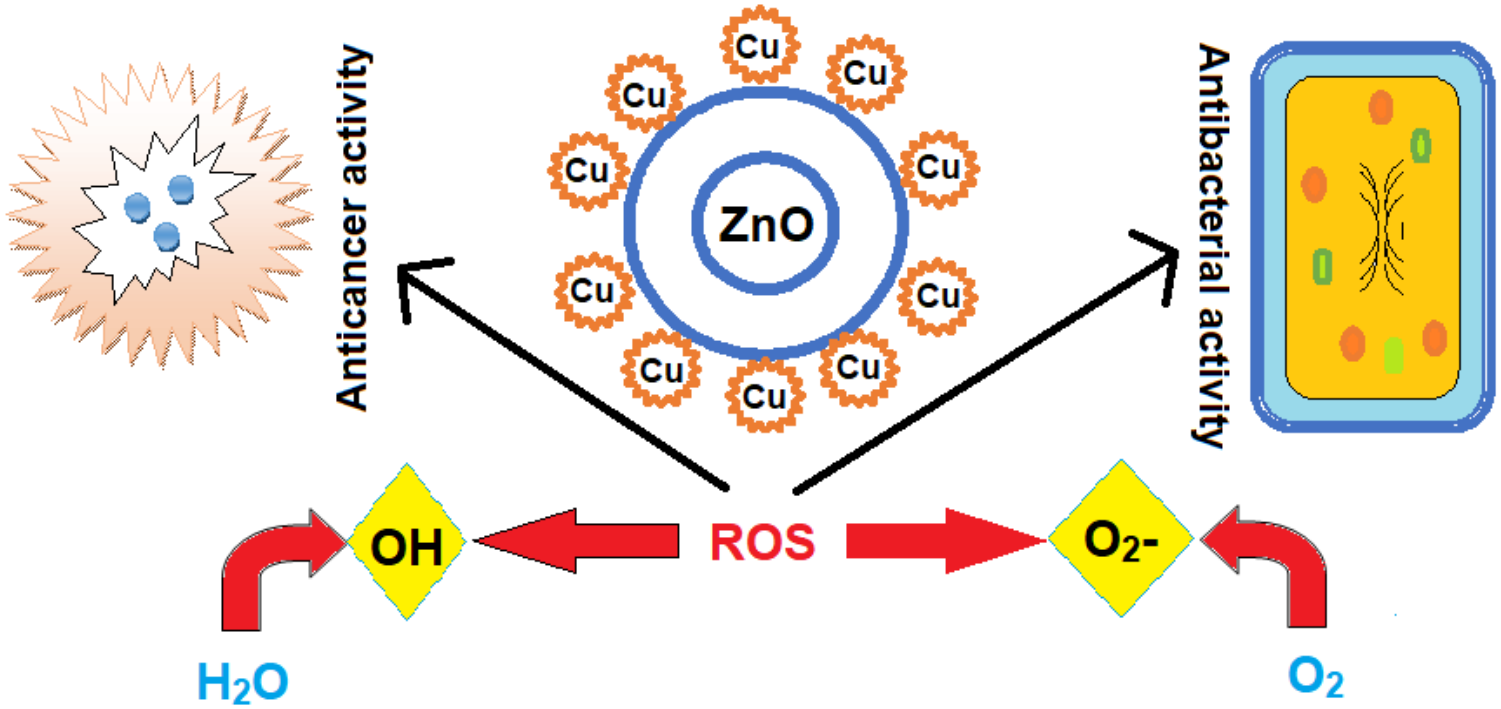

Fig 1: Graphical representation of Cu/ZnO nanocomposite for antibacterial and anticancer activity

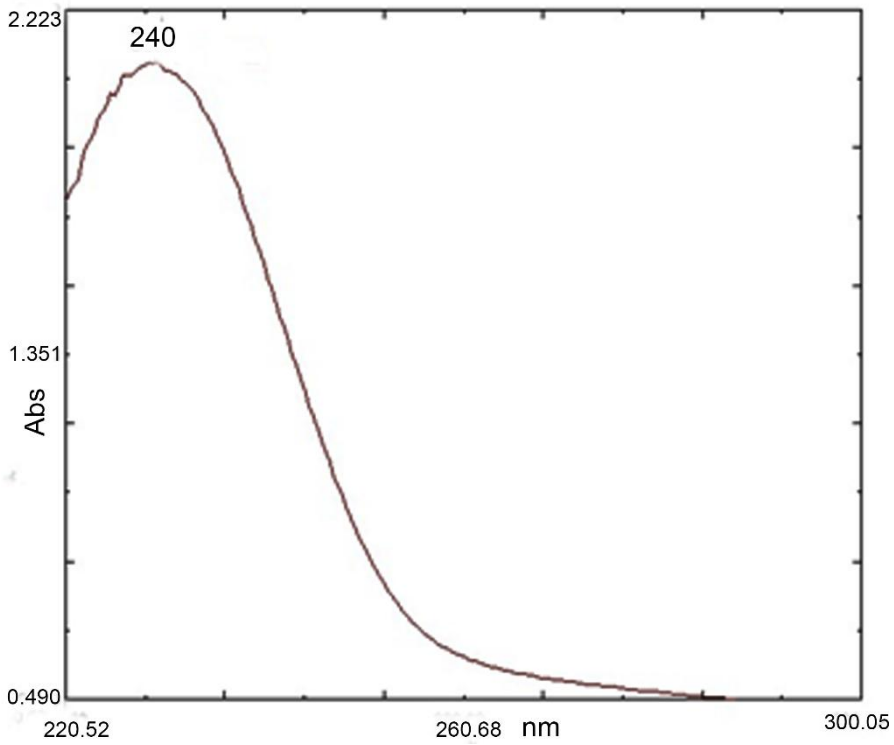

Fig.2: UV spectrum of *L. aculeate* mediated Cu/ZnO nanocomposite observed peak at 240 nm.

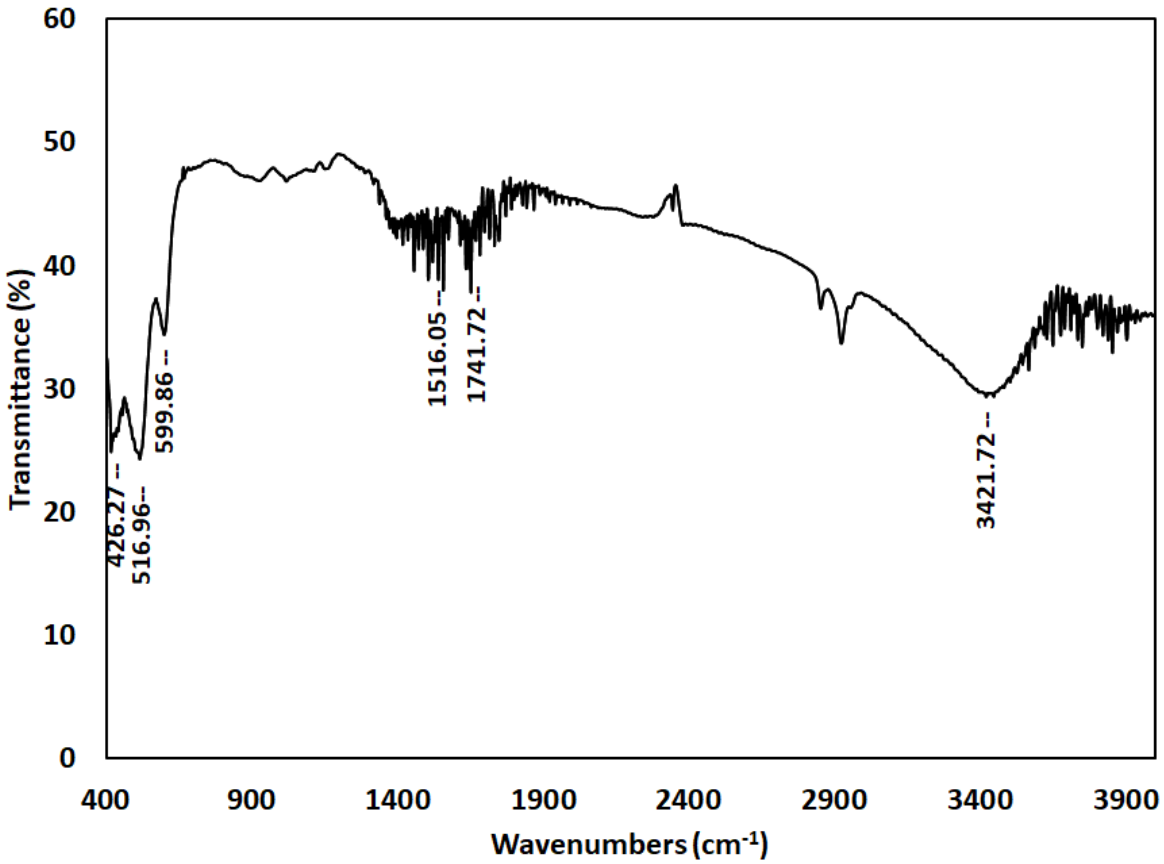

Fig.3: FTIR spectrum of *L. aculeata* mediated Cu/ZnO nanocomposite

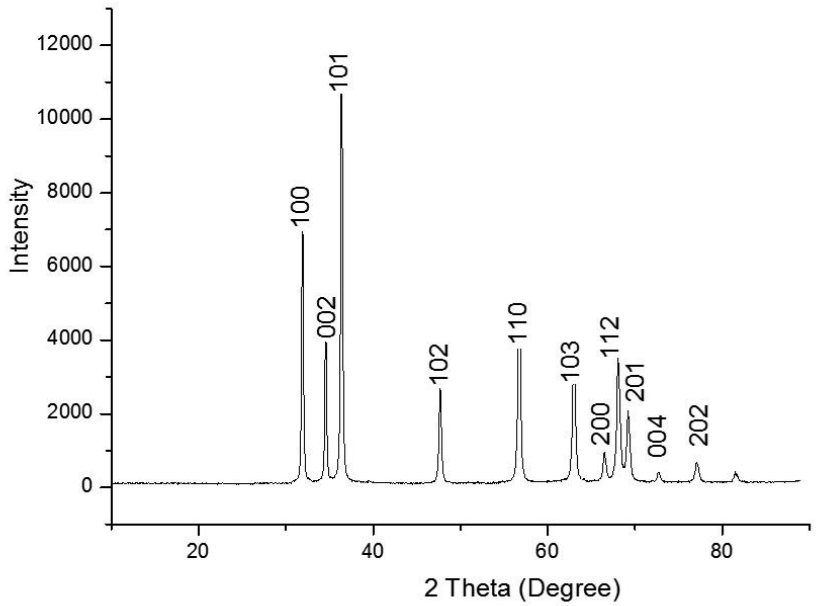

Fig.4: XRD spectrum of *L. aculeate* mediated Cu/ZnO nanocomposite

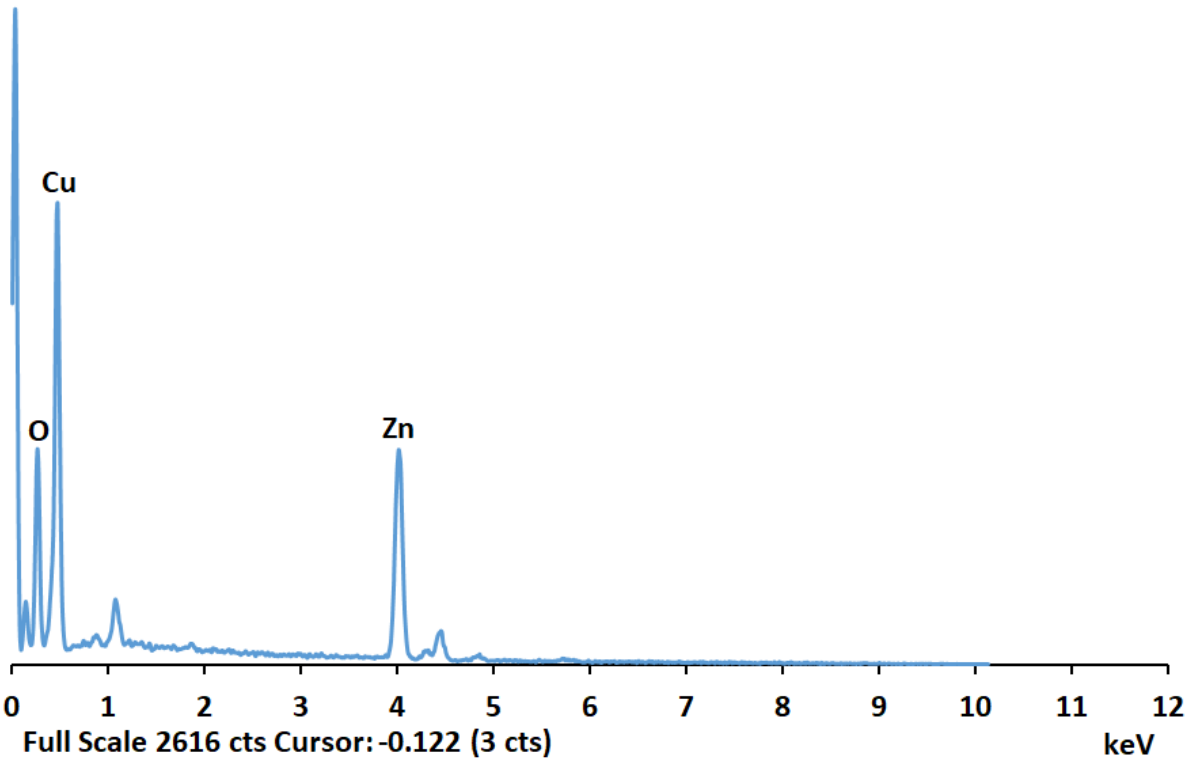

Fig.5: EDX spectrum of *L. aculeate* mediated Cu/ZnO nanocomposite

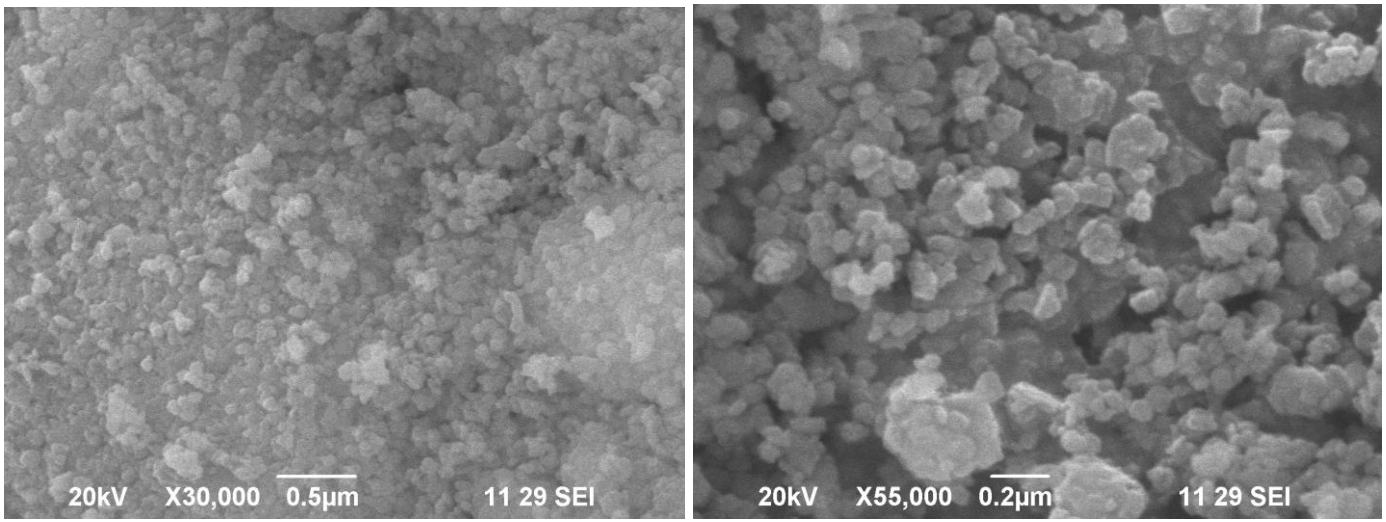

Fig.6: SEM images of *L. aculeate* mediated Cu/ZnO nanocomposite

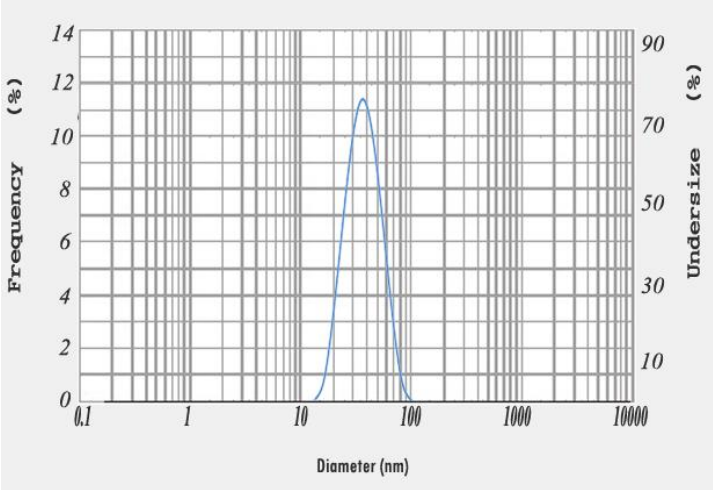

Fig 7: Particle size analysis of Cu/ZnO nanocomposite

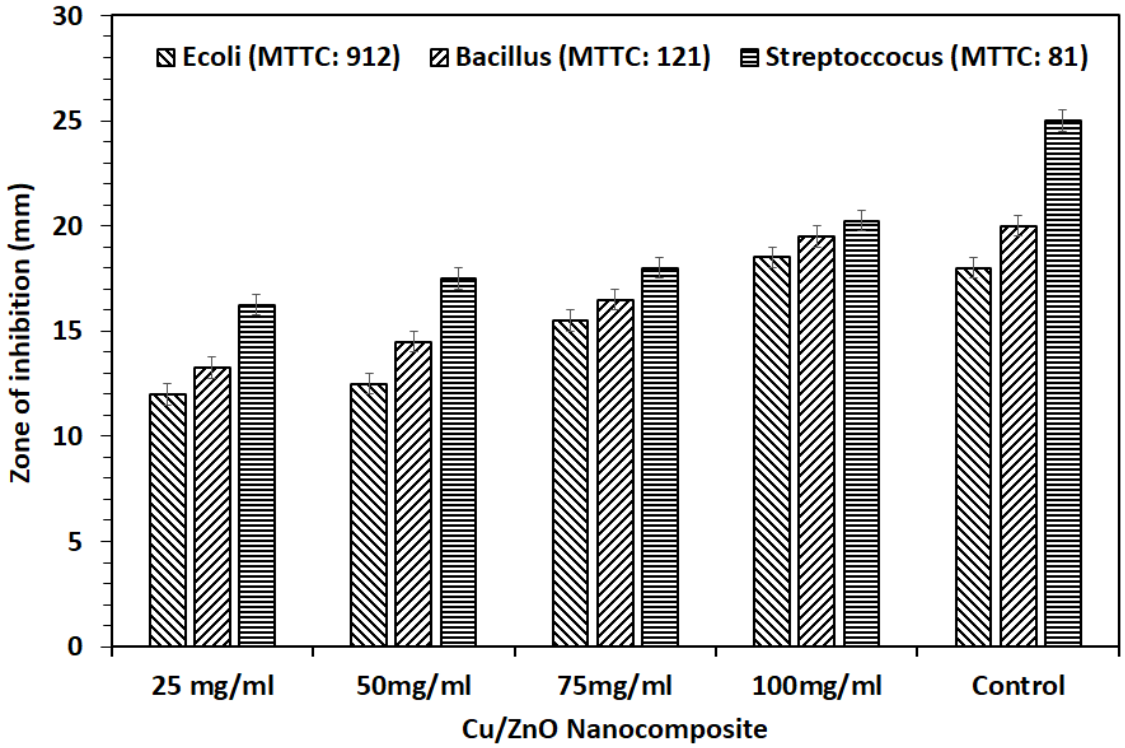

Fig 8: Antibacterial activity of Cu/ZnO nanocomposite by well diffusion assay. The results are expressed as mean ± SD

Table 1 Antioxidant activity of Cu/ZnO nanocomposite. All the results are statistically significant (*P* value ≤ 0.05) using t test

Nanocomposite concentration (mg/ml)	Mean	Std Deviation	Std Error Mean	t	Sig (t-tailed)
25	20.83	0.76	0.44	47.24	0.000
50	58.41	0.38	0.22	264.95	0.000
75	72.00	0.25	0.14	498.83	0.000
100	80.75	0.66	0.38	211.45	0.000

Table 2 Anova analysis of variance for the data on inhibition zone of Cu/ZnO nanocomposite against bacteria pathogen. All the results are statistically significant (*P* value ≤ 0.05) using Tukey test

Nanocomposite concentration (mg/ml)		Sum of square	Mean Square	F	Sig.
25	Between Pathogen	76.272	25.424	326.299	0.000
	With pathogen	0.623	0.078		
	Total	76.896			
50	Between Pathogen	115.684	38.561	284.761	0.000
	With pathogen	1.083	0.135		
	Total	116.767			
75	Between Pathogen	78.462	26.154	132.008	0.000
	With pathogen	1.585	0.198		
	Total	80.047			
100	Between Pathogen	10.981	3.660	14.354	0.001
	With pathogen	2.040	0.255		
	Total	13.021			

Table 3 *In vitro* anti-proliferative effect of *Lantana aculeate* mediated Cu/ZnO nanocomposite on SiHa cell lines by MTT assay

Cu/ZnO Nanocomposite concentration (µg/ml)	Average absorbance (nm)	Percentage viability (%)
6.25	0.28	81.45
12.5	0.25	69.76
25	0.23	65.63
50	0.22	61.04
100	0.20	53.51